Flightless anchors IQGAP1 and R-ras to mediate cell extension formation and matrix remodeling

P. D. Arora[a,*], K. Nakajima[a], A. Nanda[a], A. Plaha[a], A. Wilde[b], D. B. Sacks[c], and C. A. McCulloch[a]
[a]Faculty of Dentistry, University of Toronto, Toronto, ON M5G 1G6, Canada; [b]Departments of Medical Genetics and Biochemistry, Faculty of Medicine, University of Toronto, Toronto, ON M5G 1L7, Canada; [c]Department of Laboratory Medicine, National Institutes of Health, Bethesda, MD 20892

ABSTRACT **Tractional remodeling of collagen fibrils by fibroblasts requires long cell extensions that mediate fibril alignment. The formation of these cell extensions involves flightless I (FliI), an actin-binding protein that contains a leucine-rich-repeat (LRR), which binds R-ras and may regulate cdc42. We considered that FliI interacts with small GTPases and their regulators to mediate assembly of cell extensions. Mass spectrometry analyses of FliI immunoprecipitates showed abundant Ras GTPase-activating-like protein (IQGAP1), which in immunostained samples colocalized with FliI at cell adhesions. Knockdown of IQGAP1 reduced the numbers of cell extensions and the alignment of collagen fibrils. In experiments using dominant negative mutants, cdc42 activity was required for the formation of short extensions while R-ras was required for the formation of long extensions. Immunoprecipitation of wild-type and mutant constructs showed that IQGAP1 associated with cdc42 and R-ras; this association required the GAP-related domain (1004–1237 aa) of IQGAP1. In cells transfected with FliI mutants, the LRR of FliI, but not its gelsolin-like domains, mediated association with cdc42, R-ras, and IQGAP1. We conclude that FliI interacts with IQGAP1 and co-ordinates with cdc42 and R-ras to control the formation of cell extensions that enable collagen tractional remodeling.**

Monitoring Editor
Laurent Blanchoin
CEA Grenoble

Received: Oct 4, 2019
Revised: May 6, 2020
Accepted: May 11, 2020

INTRODUCTION

In fibrous connective tissues, fibroblasts are the predominant cells that synthesize and remodel collagen fibers to maintain tissue homeostasis. Imbalances of extracellular matrix (ECM) remodeling are associated with several diseases including congenital disorders (e.g., heart valve malformations), organ fibrosis, invasive cancers, and ankylosis of joints or teeth (Bonnans *et al.*, 2014). To enable ECM remodeling by traction, fibroblasts attach to matrix proteins using adhesion receptors such as integrins (e.g., $\alpha 2\beta 1$, $\alpha 11\beta 1$) and the discoidin domain receptor 2. For remodeling of collagen fibrils in vivo, fibroblasts undergo marked changes in cell shape that involve the generation of long cell extensions, which enable collagen fiber remodeling (Melcher and Chan, 1981). Plasma membrane extensions, including spike-like filopodia and broader, fan-shaped lamellipodia, are generated through the organization and remodeling of actin filaments, which in turn are regulated by a large array of actin-binding proteins and associated signal modules including small GTPases. These extensions in turn play critical roles in the remodeling of ECM proteins like collagen (Everts *et al.*, 1996).

Filopodia adhere to the substratum through integrin-based focal complexes (Nobes and Hall, 1995; Geiger *et al.*, 2009) and in NIH 3T3 cells their formation is dependent on cdc42 (Ridley *et al.*, 1992). While the regulation of filopodia by cdc42 is well established (Ohta *et al.*, 1999; Dimchev *et al.*, 2017), the involvement of other GTPases and their role in the formation of longer cell extensions are not well defined. One member of the Ras family of GTPases, R-ras, mediates a diverse range of cellular processes involving cytoskeletal rearrangements such as the generation of cell extensions, adhesion, migration and phagocytosis (Keely *et al.*, 1999; Self *et al.*, 2001; Kwong *et al.*, 2003; Arora *et al.*, 2018). Small GTPases like R-ras exist in inactive GDP-bound and active GTP-bound states that are regulated by guanine nucleotide exchange factors, which promote conversion

This article was published online ahead of print in MBoC in Press (http://www.molbiolcell.org/cgi/doi/10.1091/mbc.E19-10-0554) on May 20, 2020.

Author contributions: P.A. and C.M. designed research; P.A., K.N., A.N., and A.P. performed research; D.S. contributed new reagents; P.A., K.N., A.N., and A.P. analyzed data; P.A., A.N., A.W., D.S., and C.M. wrote the paper.

*Address correspondence to: Pamma Arora (pam.arora@utoronto.ca).

Abbreviations used: DN, dominant negative; ECM, extracellular matrix; FBS, fetal bovine serum; FliI, Flightless I; GLD, gelsolin-like domain; GRD, GAP-related domain; IQGAP1, Ras GTPase-activating-like protein; KND, knockdown; LRR, terminal leucine-rich-repeat; PBS, phosphate-buffered saline; ROI, region of interest; TBS, Tris-buffered saline; WT, wild type.

from a GDP-bound to a GTP-bound state, and by GTPase-activating proteins, which accelerate the hydrolysis of GTP to GDP. These regulators ensure that the activation and inactivation of GTPases are controlled spatio-temporally to generate specific, localized responses (Hall, 1998; Kaibuchi *et al.*, 1999). GTP-bound Ras binds to numerous effectors (e.g., RAF, PI3K, RalGDS, Rin1, Tiam, Af6, PLCε, and PKCζ) to trigger various signaling cascades (Rajalingam *et al.*, 2007), which in turn modulate a broad range of cellular processes including proliferation, survival, migration, differentiation, and death.

Ras GTPase-activating-like protein (IQGAP1) is a multidomain protein critically involved in a broad array of biological processes including intercellular adhesion, cell migration, growth factor signaling and cancer metastasis (Noritake *et al.*, 2005; Bourguignon *et al.*, 2005; Hayashi *et al.*, 2010; Brown and Sacks, 2006). IQGAP1 stabilizes the active (GTP-bound state) of cdc42, thereby increasing its intracellular concentration and stimulating filopodia formation (Swart-Mataraza *et al.*, 2002). In addition, IQGAP1 is required for localizing cdc42 to the plasma membrane, which links its activity to subcortical actin assembly. Distinct structural regions of IQGAP1 mediate its scaffolding functions (Jacquemet and Humphries, 2013), which facilitate the assembly of protein complexes required for signal transduction. Currently, it is not known how IQGAP1, when sequestered in adhesions, enables regulation of small GTPases involved in the generation of cell extensions.

A broad array of actin-binding proteins (e.g., fascin) are highly expressed in transformed cells to enable generation of membrane protrusions that promote increased cell motility in invasive cancers. Flightless I (FliI) is an actin capping and actin severing protein that has been suggested to play a central role in the generation of cell extensions (Arora *et al.*, 2015). Originally identified in *Drosophila melanogaster*, FliI is a conserved member of the gelsolin superfamily of proteins, which are responsible for actin filament remodeling and rearrangements of cytoskeletal architecture (Campbell *et al.*, 1993; Kwiatkowski, 1999). FliI consists of six gelsolin-like domains (GLDs), which confer actin capping and severing activities; but FliI also contains an N-terminal leucine-rich-repeat (LRR) (Campbell *et al.*, 1997). The presence of an LRR domain in FliI may enable interactions with other essential proteins involved in the regulation of the actin cytoskeleton to mediate cell extension formation and ECM remodeling (Kopecki and Cowin, 2008). FliI is enriched at nascent cell–matrix adhesions in fibroblasts (Mohammad *et al.*, 2012) and colocalizes with Ras (Davy *et al.*, 2001). More recent data show that R-ras associates with FliI through the N-terminal LRR domain of FliI, an interaction that enables the generation of plasma membrane extensions in fibroblasts by an unknown mechanism (Arora *et al.*, 2018). Here we considered that FliI acts as an adaptor protein to bind IQGAP1; FliI and IQGAP1 then co-ordinate with cdc42 and R-ras to control the formation of cell extensions. The formation of these extensions is important for the remodeling of high abundance proteins like collagen in the ECM (Melcher and Chan, 1981).

RESULTS

IQGAP1 associates with FliI

We investigated the molecular mechanisms by which FliI regulates cell extension formation. FliI-interacting proteins were first identified in immunoprecipitates prepared from 3T3 cells that expressed FliI (FliI wild type [WT]) or in FliI siRNA-silenced 3T3 cells (FliI KND). FliI immunoprecipitates examined by mass spectrometry showed that FliI associated with IQGAP1 (Table 1). As IQGAP1 is a scaffolding protein that integrates signals from cdc42 to promote filopodia development, we considered that the association of FliI with IQGAP1 enables coordination with cdc42 and R-ras to control cell extension formation from nascent filopodia.

We assessed whether IQGAP1 was the only IQGAP isoform expressed by FliI WT cells. By immunoblotting we found that FliI WT and KND cells expressed IQGAP1 but not IQGAP2 or IQGAP3 (Supplemental Figure S1A). Lysates from HEPG2 cells and placenta extracts were used as positive controls for IQGAP2 and IQGAP3, respectively.

We determined whether the FliI-IQGAP1 association was dependent on the formation of cell adhesions to the ECM. Accordingly, FliI WT cells were plated on collagen or were deprived of adhesion to the matrix by maintaining cells in suspensions. Analysis of FliI immunoprecipitates showed fivefold enhanced association between FliI and IQGAP1 in attached cells compared with cells maintained in suspensions or of cells that were immunoprecipitated with a control antibody (Figure 1A). In experiments using IQGAP1 immunoprecipitation of FliI WT cells followed by immunoblotting for FliI, there was 2.5-fold greater association between IQGAP1 and FliI in attached cells versus suspended cells or of cells that were immunoprecipitated with a control antibody (Figure 1B).

We examined whether integrin engagement enabled colocalization of FliI and IQGAP1 in cell extensions. In FliI WT cells plated on collagen, immunostaining showed moderate colocalization of FliI with IQGAP1 in cell adhesions that localized to the edges of cells (Figure 1C). Based on quantitative analysis (Pearson colocalization) of regions of interest (ROI) at cell peripheries that lay beneath the subcortex and included cell adhesions, there was >2-fold greater colocalization of FliI and IQGAP1 in cells plated on collagen than in cells plated on poly-L-lysine ($p < 0.01$). Further, when plated on collagen substrates, FliI KND cells did not exhibit colocalization of IQGAP1 with the focal adhesion marker vinculin at cell edges and

Protein name	Accession number	Molecular weight	FliI Ab: # of tryptic peptides	Irrelevant Ab: # of tryptic peptides
Actin, cytoplasmic	ACTG_mouse	42 kDa	1376	794
Vimentin	VIME_mouse	54 kDa	568	512
Myosin-9	MYH9_9-mouse	226 kDa	218	110
Ras-GTPase-activating protein SH3 domain-binding protein (G3BP1)	G3BP1_mouse	52 kDa	87	49
Rho GTPase-activating protein 22	RHG21_mouse	78 kDa	59	29
Ras GTPase-activating-like protein IQGAP1	IQGA1_mouse	189 kDa	21	11
Rac GTPase-activating protein	RGAP1_mouse	239 kDa	20	17

TABLE 1: Mass spectrometry analysis of FliI immunoprecipitates.

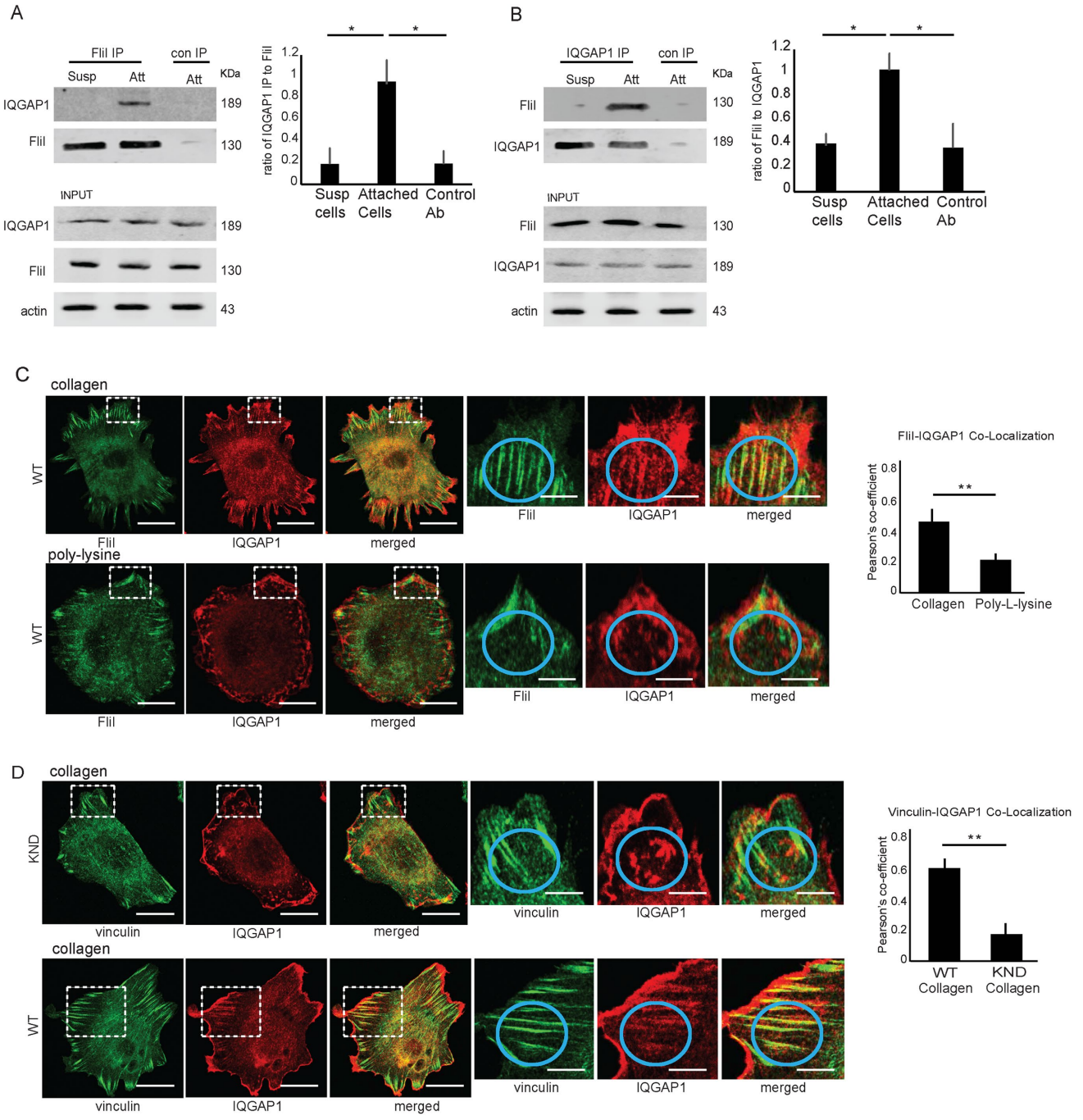

FIGURE 1: Association of FliI with IQGAP1 and effect of cell adhesion to collagen. (A) FliI WT cells were plated on collagen for 3 h (attached) or were maintained in suspension (Susp) to examine the effect of adhesion to collagen on the association of FliI with IQGAP1. Cell lysates were immunoprecipitated with FliI antibody and the lysates immunoblotted for IQGAP1. A control antibody (anti-nebulin) was used to assess the specificity of the immunoprecipitation reaction. Densitometry of immunoblots shows fivefold enhanced association between FliI and IQGAP1 compared with cells in suspension or by immunoprecipitation with the control antibody (*$p < 0.05$). Experiments were repeated three times. (B) Same experimental approach as A, except lysates were immunoprecipitated with IQGAP1 antibody and immunoblotted for FliI. Densitometry shows 2.5-fold increased association of IQGAP1 and FliI in attached cells compared with lysates immunoprecipitated with control antibody or preparations from suspended cells (*$p < 0.05$; $n = 3$). (C) Panels on left show representative images of FliI WT cells plated on collagen or poly-L-lysine for 3 h. Cells were co-immunostained for FliI and IQGAP1. Bar, 10 μm. Panels on right side are higher power magnifications from dotted line square boxes depicted on left side images. Bar, 4 μm. For colocalization analysis, Pearson's correlation coefficient was computed for image pairs of immunostained IQGAP1 and FliI or IQGAP1 and vinculin in WT cells (ImageJ). Data reported are mean ± SD from 50 cells for each condition (*$p < 0.01$ between two groups). Blue circles indicate sites for colocalization analysis on pairs of images. (D) Same experimental approach as for panels in C, except that cells were co-immunostained for vinculin (a focal adhesion marker) and IQGAP1 (*$p < 0.01$ between two groups; $n = 50$ cells). Blue circles indicate sites for colocalization analysis on pairs of images.

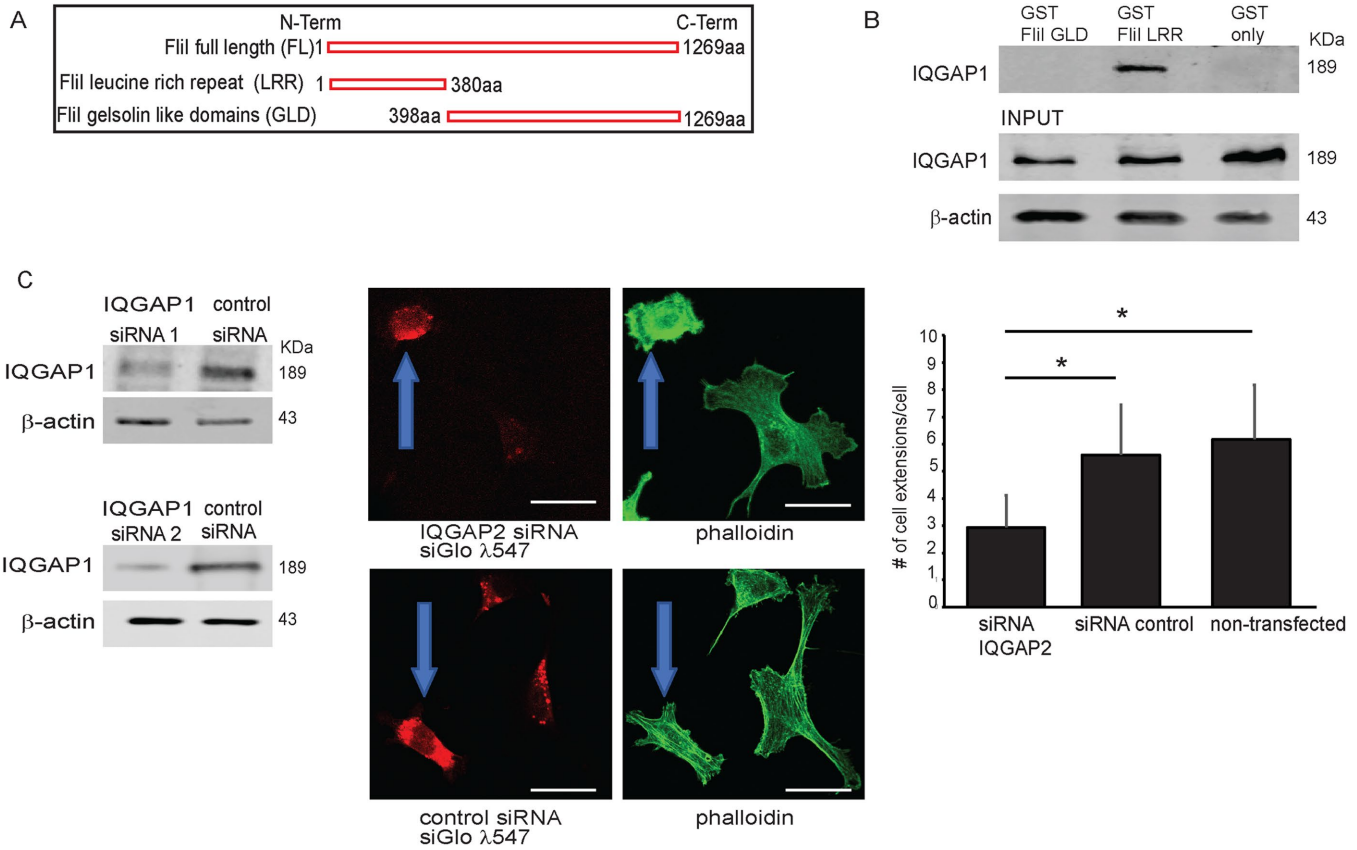

FIGURE 2: Interaction of Flil LRR with IQGAP1. (A) Diagram of domain structure of Flil showing the C-terminal GLDs and the N-terminal LRR. (B) Pull-down assay shows proteins eluted from GST only, GST Flil GLD, and GST-Flil-LRR Sepharose beads incubated with Flil WT cell lysates. There is abundant IQGAP1 protein bound to the GST Flil LRR beads but no detectable IQGAP1 is bound to the GST only or GST Flil GLD beads. Equal amounts of proteins were loaded on beads (INPUT). These experiments were repeated four times. (C) KND of IQGAP1expression with two different siRNAs (siRNA 1, siRNA 2) that show 70 and 78% reduction of IQGAP1 protein levels. Confocal images of Flil WT cells transiently cotransfected with IQGAP1 siRNA 2 and fluorescent dye (siGloDY-547; to identify transfected cells) show twofold reduction in number of cell extensions compared with nontransfected Flil WT or cells transfected with control siRNA (*$p < 0.05$). Data shown in histograms are from three different experiments. Data are reported as mean ± SD, analyzed by ANOVA. Blue arrows show same cell in matching panels that were transfected with siRNAs.

IQGAP1 instead became more abundant in subcortical sites of cell protrusions. In comparison, Flil WT cells showed threefold higher colocalization of IQGAP1 with vinculin ($p < 0.01$; Figure 1D). In the absence of Flil, the localization of vinculin in collagen adhesions was poorly aligned and short cell extensions were not as well developed, indicating that Flil in cell adhesions plays an important role in driving cell extension formation. These differences were not attributable to variations of IQGAP1 abundance as Flil WT and KND cells exhibited similar expression levels of IQGAP1 (Supplemental Figure S1B).

IQGAP1 interacts with the LRR of Flil and regulates cell extension formation

The LRR of Flil mediates its interactions with other proteins (Kobe and Kajava, 2001). Accordingly, we examined whether IQGAP1 specifically interacts with the LRR region or the GLD of Flil (Figure 2A). Experiments were conducted with GST only, GST-Flil-GLD, or GST-Flil-LRR proteins expressed in bacterial expression vectors and bound to glutathione beads. Cell lysates incubated with washed beads showed a strong association of IQGAP1 with the Flil-LRR domain but not with the other proteins (Figure 2B).

As a major function of the Rho GTPases is the regulation of actin filament assembly, which is directly involved in the formation of cell extensions (Hall, 2005), and we examined the role of IQGAP1 in cell extension formation. Cells were transfected with two different IQGAP1 siRNAs and were cotransfected with fluorescent siGlo DY-547 to identify those cells with IQGAP1 knockdown (KND). Immunoblotting for IQGAP1 followed by densitometry analysis and adjusted for β–actin showed that for siRNA 2, there was a 70 ± 9% (mean ± SD; 5 replicates) reduction of IQGAP1 protein levels and for siRNA 2, a 78 ± 9% reduction of IQGAP1 protein levels (Figure 2C). Compared with control siRNA-transfected cells, Flil WT cells transfected with IQGAP siRNA2 and also stained with siGlo DY-547 exhibited twofold fewer numbers of rhodamine phalloidin-stained cell extensions than control siRNA-transfected cells (Figure 2C, right panels).

IQGAP1 interacts with R-ras and cdc42 to drive cell extension formation

IQGAP1 is implicated in cytoskeletal function as it oligomerizes and cross-links actin filaments and augments the GTPase activity of cdc42 (Swart-Mataraza *et al.*, 2002). For studying the role of IQGAP1 in cdc42 and R-ras activation, we examined IQGAP+/+ and IQGAP1–/– mouse embryonic fibroblasts (MEFs) (Ren *et al.*, 2007). R-ras, cdc42, and Flil were all expressed in these cells

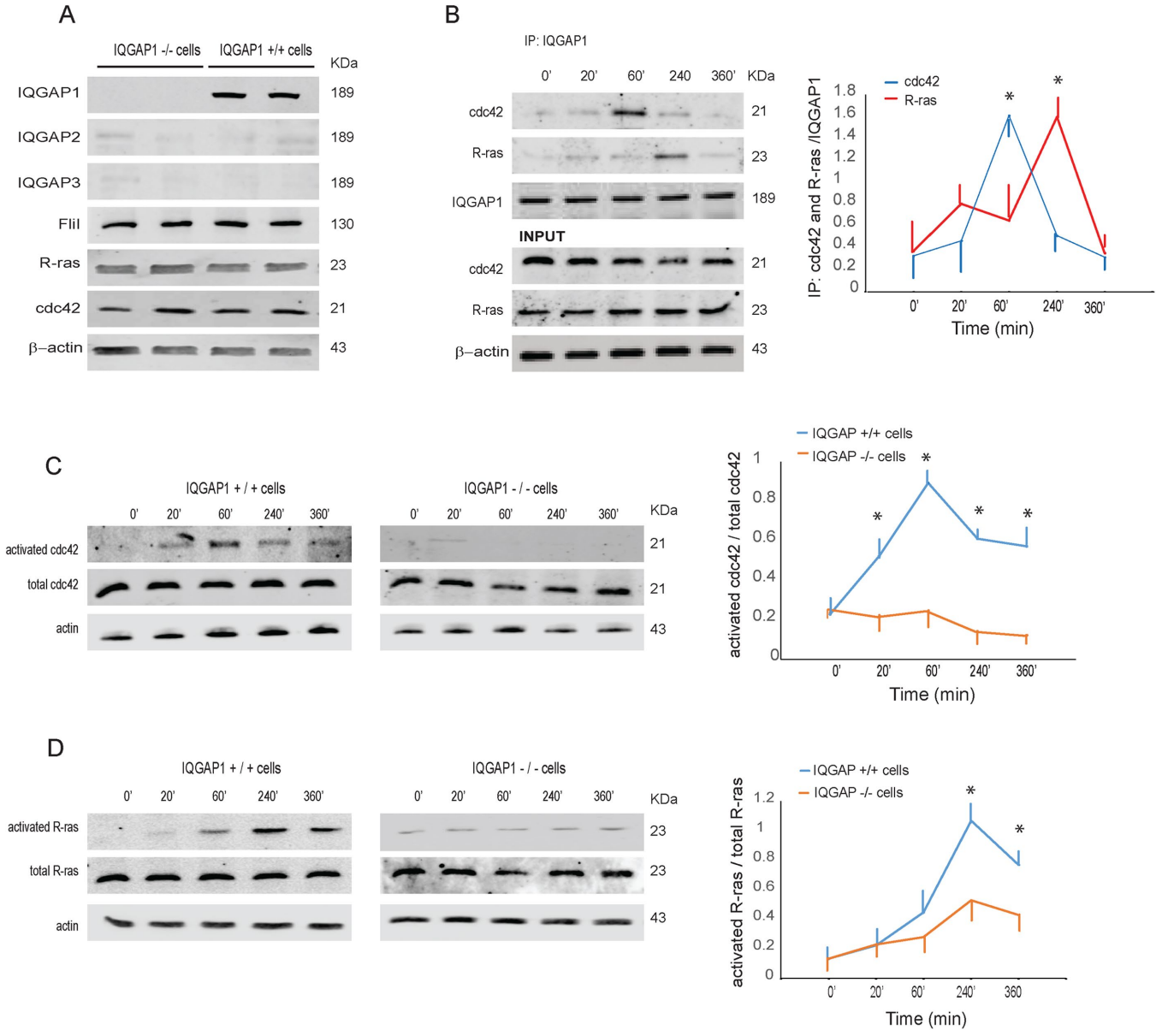

FIGURE 3: Association of IQGAP1 with cdc42 and R-ras. (A) Expression levels of Flil, R-Ras, cdc42, IQGPA2, and IQGAP3 in IQGAP1–/– and IQGAP1+/+ cells. Note that IQGAP2 and IQGAP3 are not expressed in these cells. (B) Time-dependent associations of IQGAP1 with cdc42 and R-ras were measured in IQGAP1+/+ cells plated on collagen-coated tissue culture plates over 0 min (suspended cells) and up to 360 min after plating. Cell lysates were immunoprecipitated for IQGAP1, which were immunoblotted for cdc42 and R-ras. Densitometric analysis of immunoprecipitated cdc42 and R-ras were adjusted for IQGAP1 and the time course data are shown in the line plot (right panel). Data are mean ± SD of four independent samples. Abundance of cdc42 and R-ras were different at 60 and 360 min (*$p < 0.01$ by ANOVA). (C) IQGAP1+/+ cells and IQGAP1–/– cells were plated on collagen from 0 to 360 min. Activated cdc42 and total cdc42 were measured as described in *Materials and Methods* and the ratios of their densities are plotted and displayed in right panel. Data are mean ± SD of three independent samples. Differences between IQGAP1+/+ cells and IQGAP1–/– cells indicated are *$p < 0.01$ by ANOVA. (D) Similar analysis for activated R-ras and total R-Ras were conducted as described for C. Data are from three independent experiments.

(Figure 3A). As expected, IQGAP1 was absent in IQGAP1–/– cells; IQGAP2 and IQGAP3 were not detectable in IQGAP1+/+ or IQGAP1–/– cells (Figure 3A). For assessing a potential role for IQGAP1 in the formation of cell extensions, we looked for an association between IQGAP1 and cdc42 or R-ras in IQGAP1+/+ cells that had been plated on collagen over a time course. Immunoblotting of IQGAP1 immunoprecipitates showed that IQGAP1 associated with cdc42 at 60 min and that IQGAP1 associated with R-ras by 240 min (Figure 3B). In an experiment of similar design, IQGAP1+/+ type cells plated on collagen showed activation of cdc42 and R-ras between 20 and 360 min but there was minimal cdc42 activation (Figure 3C) or R-ras activation (Figure 3D) in IQGAP1–/– cells. Quantification of these data showed there was fourfold higher activation of cdc42 (at 60 min) and 2.5-fold higher activation of R-ras (at 120 min) in IQGAP1+/+ cells compared with IQGAP1–/– cells.

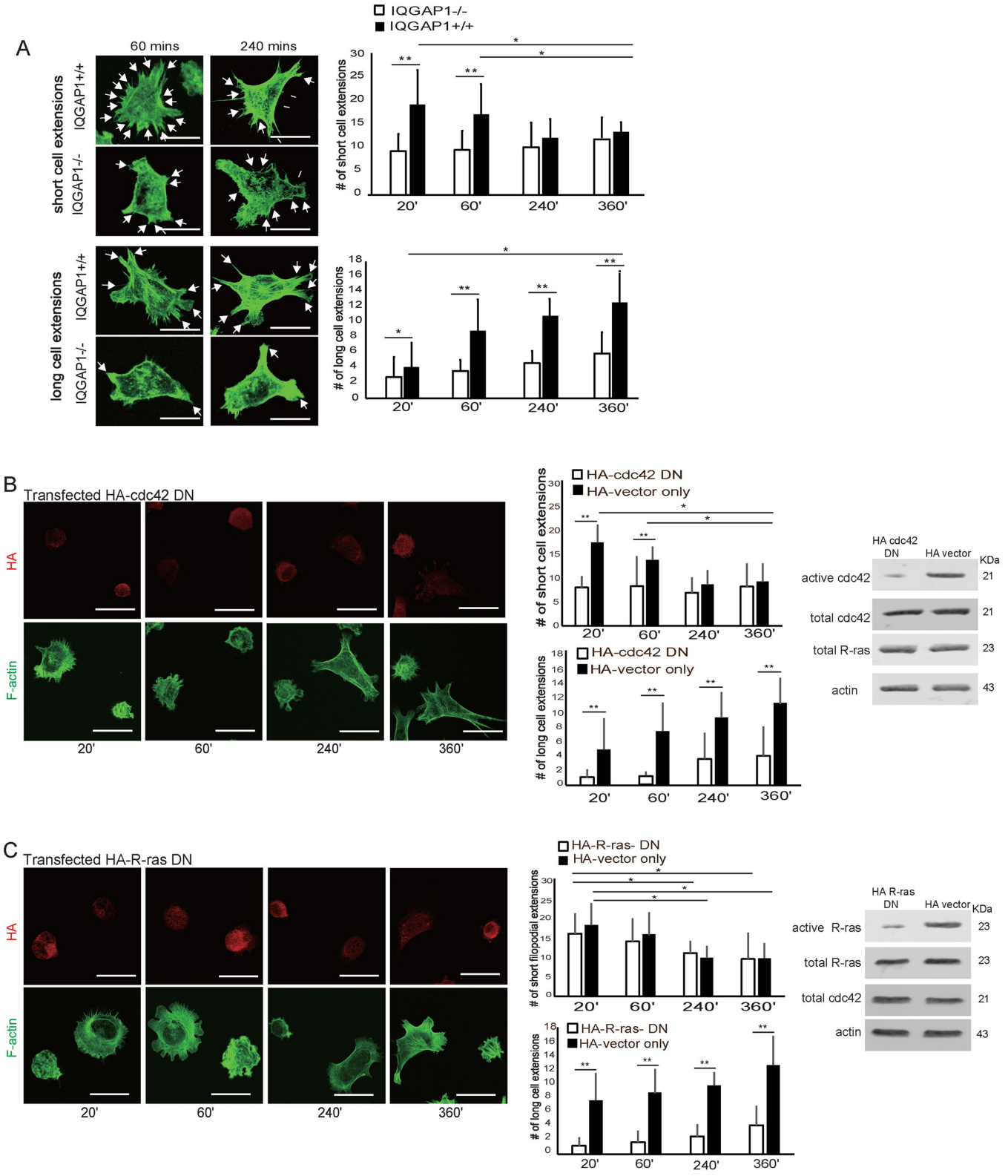

FIGURE 4: Effect of IQGAP1 expression on cell extension formation. (A) Representative images of IQGAP1+/+ and IQGAP1–/– cells showing short and long cell extensions (indicated by arrowheads) at 60 and 240 min after plating on collagen. The histograms in the panels at right show mean ± SD of number of short and long cell extensions per cell as operationally defined in *Materials and Methods*. Cells were fixed at indicated times, stained with Alexa 488 phalloidin, and imaged by confocal microscopy. Thirty cells were sampled for each group and data were analyzed by ANOVA. *$p < 0.05$; **$p < 0.01$. Scale bar, 10 μm. (B) Images of IQGAP1+/+ cells were transiently transfected with HA-cdc42 DN and a control HA empty vector was plated on collagen-coated glass for indicated times, fixed, and immunostained for HA to identify transfected cells for quantification. Cells were counterstained with Alexa 488 phalloidin. Scale bar,

We examined the involvement of IQGAP1 in the development of short and long cell extensions in IQGAP1+/+ cells plated on collagen for 60 and 360 min. We first characterized the cell protrusions and localized nascent adhesions by immunostaining for talin; MYO-10 was used as a cell extension tip marker. We operationally defined short extensions as protrusions from the plasma membrane of 1–4.5 μm in length. The longer cell extensions were also immunostained for MYO-10 and we designated long extensions as protrusions from the plasma membrane of >4.5 μm in length (Supplemental Figure S1C). With these operational definitions, we compared the number of short and long extensions in IQGAP1+/+ and IQGAP1–/– cells that were plated on collagen, fixed and stained with MYO-10 and phalloidin. Quantification of confocal images indicated that in comparison with IQGAP1–/– cells, IQGAP1+/+ cells exhibited twofold more numerous short extensions per cell ($p < 0.01$) that formed more rapidly (in the first 20–60 min after plating) and which gradually subsided to similar numbers as were seen for IQGAP1–/– cells by 240–360 min ($p > 0.2$; Figure 4A). In contrast, the number of short extensions formed by IQGAP1–/– cells did not increase over time (Figure 4A). In IQGAP1+/+ cells the number of long cell extensions progressively increased over time (fourfold more extensions at 360 min compared with 20 min, $p < 0.01$). Further, there were fewer long extensions in IQGAP1–/– cells and the number of long extensions did not change over time after plating ($p > 0.2$; Figure 4A).

We studied the roles of cdc42 and R-ras in the development of small and long cell extensions by transfecting IQGAP1+/+ cells with dominant negative (DN) HA-tagged cdc42, HA-R-ras DN or control HA-only vector. Confocal images of control HA-only vector-transfected cells showed moderate numbers of short cell extensions at 20– 60 min after plating that progressively decreased from 60 to 360 min ($p < 0.01$; Figure 4B). Cells transfected with HA-DN cdc42 showed greatly reduced ($p < 0.01$) numbers of short extensions compared with controls and these numbers were unchanged over time after plating (Figure 4B). We also examined the effect of DN-cdc42 on the formation of long cell extensions. Control cells showed time-dependent increases in the number of long cell extensions ($p < 0.01$), whereas cells transfected with HA-cdc42-DN exhibited reduced numbers of extensions that remained unchanged over time (Figure 4B). These data suggest that shortly after plating, cdc42 is required for the formation of short extensions and later for the formation of longer cell extensions (i.e. operationally defined as > 4.5 μm). Lysates prepared from HA-cdc42-DN and HA-vector-only transfected cells (four different cultures each) that had been plated on collagen were immunoblotted and the blots were examined for cdc42 and R-ras. These data showed that as expected, HA-cdc42 DN inhibited cdc42 activation (active cdc42:total cdc42 ratio data; for DN group, 0.07 ± 0.03; for HA vector group, 0.92 ± 0.08; $n = 4$; $p < 0.01$) but did not affect the expression of R-ras (Figure 4B; right panel).

IQGAP1+/+ cells transfected with HA-R-ras-DN or control HA-empty vector were used to examine the role of R-ras in cell extension formation. Confocal imaging and quantification of cell extensions showed that the numbers of short cell extensions in HA-R-ras-DN-transfected cells decreased over time ($p < 0.01$ at 240 min; $p < 0.01$ at 360 min; Figure 4C). In contrast, the numbers of long cell extensions in control cells increased over time (from 20 to 360 min; $p < 0.01$), whereas HA-R-ras-DN-transfected cells exhibited greatly reduced numbers of extensions that remained unchanged over time. Immunoblotting of the lysates from HA-R-ras-DN and control HA-empty vector-transfected cells that had been plated on collagen (Figure 4C, right panel) showed that HA-R-ras DN strongly inhibited the activity of R-ras (active R-ras:total R-ras ratio data; for DN group, 0.22 ± 0.09; for HA vector group, 0.98 ± 0.10; $n = 4$; $p < 0.01$) but did not affect the expression of cdc42.

Role of IQGAP1-GAP-related domain [GRD] domain

While the domains of IQGAP1 that are required for its association with cdc42 were defined earlier (Swart-Mataraza *et al.,* 2002), the IQGAP1 domains that associate with R-ras are not known (Morgan *et al.,* 2019). IQGAP1–/– cells were transfected with GFP-tagged, full-length IQGAP1 WT or with truncated IQGAP1 mutants, namely IQGAP1 ΔIQ (745–864 aa deleted), IQGAP1 ΔGRD (1004–1237 aa deleted), IQGAP1 ΔWW (679–712 aa deleted), or GFP-empty vector (Figure 5A). Transfected cells were plated on collagen for 60 and 240 min and lysed, and the lysates were immunoprecipitated with a GFP antibody and separated by 10% SDS–PAGE. We selected plating times of 60 and 240 min because the data above showed that these were the time points when there would be low or maximal associations between IQGAP1 and R-ras. When the GFP immunoprecipitates were immunoblotted for R-ras, we found associations among IQGAP1, IQGAP1 ΔIQ (745–864 aa), or IQGAP1 ΔWW (679–712 aa) with R-ras at 240 min. In contrast, there was fivefold less association with the IQGAP1 ΔGRD (1004–1237 aa deletion; Figure 5A), indicating that the association of R-ras with IQGAP1 requires the GRD region of IQGAP1.

We assessed the requirement of the GRD domain of IQGAP1 for the formation of long cell extensions, which are associated with R-ras function. GFP-IQGAP1 or GFP-IQGAP1 ΔGRD was transfected into IQGAP1–/– cells, which were then plated on collagen-coated, glass-bottom dishes for 240 min. Confocal microscopy of cells transfected with GFP-IQGAP1-ΔGRD showed that these cells were rounded and did not exhibit cell extensions (Figure 5B). Quantification of these images showed eightfold reduction ($p < 0.01$) in the number of long cell extensions in cells transfected with ΔGRD IQGAP1 compared with GFP-IQGAP1 (Figure 5B).

FLil association with cdc42 and R-ras requires the GRD region of IQGAP1

As described above, IQGAP1 is required for cell extension formation, associates with the Flil-LRR (but not with the Flil-GLD; Figure 2B), and associates with cdc42 and R-ras to enable the formation of

10 μm. Histograms in the right panels show quantification of short and long cell extensions for HA-cdc42 DN-transfected or HA empty vector-transfected cells. Data are mean ± SD of the number of extensions per cell. Twenty-five cells were sampled for each group and data were analyzed by ANOVA. Differences between groups are indicated as *$p < 0.05$; **$p < 0.01$. Panel at the right shows immunoblots for active cdc42 and for indicated proteins of cell lysates prepared from transfected cells that had been plated on collagen for 20 min. (C) Left panels: representative images of cells transiently transfected with HA-R-ras DN show cells after plating on collagen for indicated time intervals. Scale bar, 10 μm. Quantification of number of short and long cell extensions shown in histograms was performed as for cells shown in B. Data are mean ± SD of number of extensions per cell. Twenty-five cells were sampled for each group and data were analyzed by ANOVA. Differences between groups are indicated as *$p < 0.05$; **$p < 0.01$. Panel at right shows immunoblots for active R-ras and for indicated proteins of cell lysates prepared from transfected cells that had been plated on collagen for 240 min.

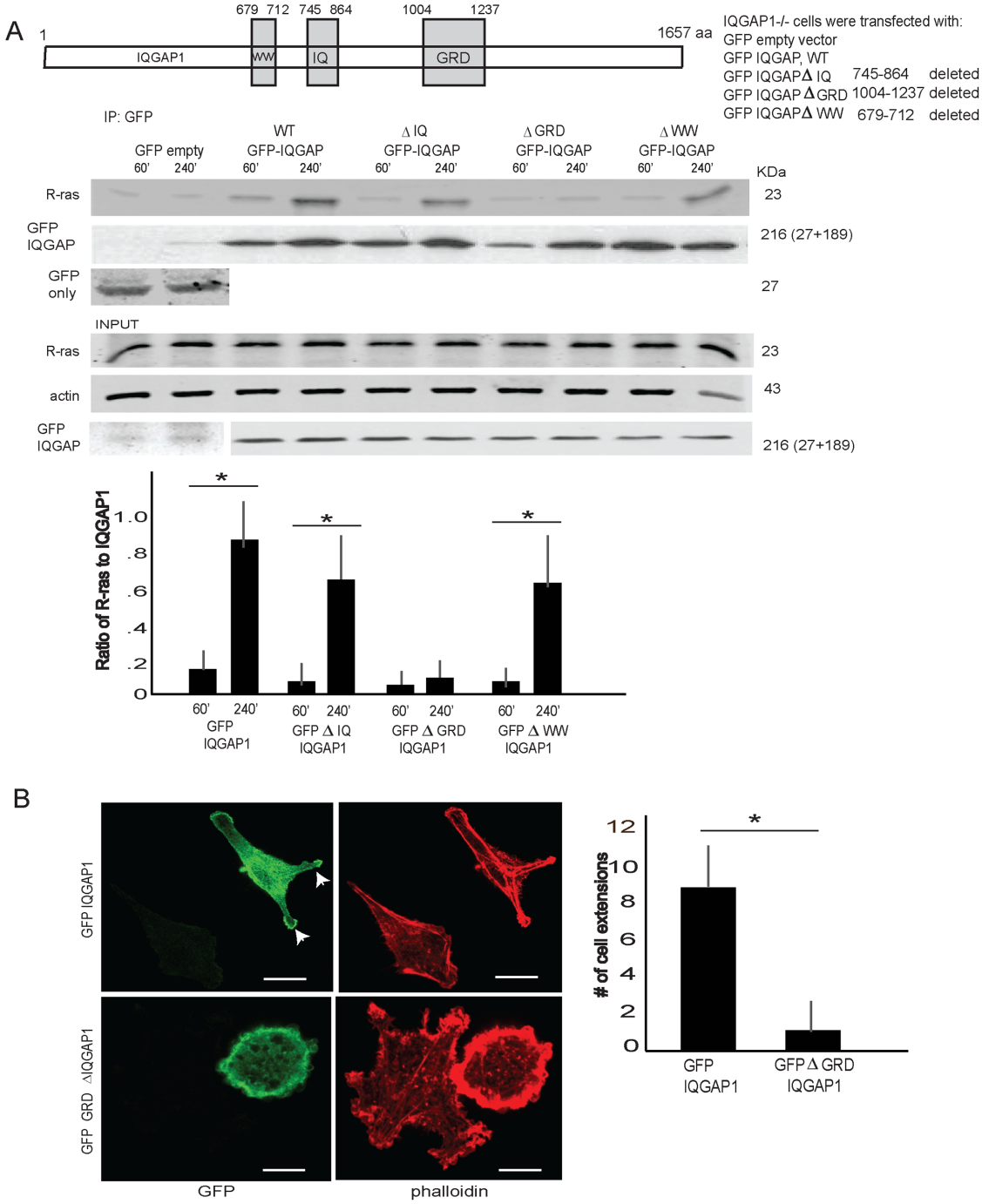

FIGURE 5: Involvement of IQGAP1 domains for association with cdc42 and R-ras. (A) Top panel shows domains of IQGAP1 deleted for studies of association with cdc42 and R-ras. Middle panel shows immunoprecipitation and immunoblotting data in which IQGAP1–/– cells were transfected with GFP-tagged WT IQGAP1, IQGAP1ΔIQ, IQGAP1ΔGRD, IQGAP1ΔWW, or with GFP empty vector. Cells were plated on collagen for 60 or 240 min. Lysates were immunoprecipitated with anti-GFP antibody. Immunoprecipitates were separated on 8% SDS–PAGE gels and immunoblotted for the indicated proteins. These gels enabled visualization of GFP empty vector (27 kDa; separate blot) and GFP-tagged IQGAP1 variants (200–216 kDa) but did not show marked differences of molecular weight between different molecular weight GFP-tagged IQGAP1 transfectants with the indicated deletions. Densitometry of indicated proteins are the ratios of R-ras to IQGAP1. Loading control immunoblots are shown below. The loading control for the GFP vector alone is shown as a separate blot with longer exposure (two left lanes). Data are mean ± SD of three independent samples. Differences between pairs of similar transfected cells plated on collagen for 60 or 240 min were analyzed by ANOVA and are indicated by *$p < 0.01$. (B) Confocal images show IQGAP1–/– cells transfected with GFP-IQGAP or GFP-IQGAP1ΔGRD, plated on collagen-coated glass for 240 min, fixed, and stained with Alexa 567-phalloidin. The number of long cell extensions (>4.5 μm) was quantified in 30 cells for each experimental condition. Analysis between two groups used Student's *t* test, which shows eightfold reduction in number of long cell extensions in cells transfected with ΔGRD truncated IQGAP1 compared with GFP-IQGAP (*$p < 0.01$).

short and long cell extensions. We considered whether FliI performs an important adaptor function by associating with IQGAP1 at growing cell protrusions, which would then enable interactions with cdc42 and R-ras to promote actin filament assembly and further elongation of cell extensions. Accordingly, we first compared the activities of cdc42 and R-ras in FliI WT and FliI KND cells in a time course after plating cells on collagen. We observed time-dependent increases of cdc42 activity, which was strongly increased at 60 min in FliI WT cells, whereas FLiI KND cells showed no significant change of activity over time ($p > 0.2$). Quantification of the blot densities showed twofold higher cdc42 activity at 60 min in FliI WT cells compared with FliI KND cells ($p < 0.01$; Figure 6A). We also observed twofold higher R-ras activity in FLiI WT cells at 240 min on collagen compared with FliI KND cells ($p < 0.01$; Figure 6A).

We assessed whether FliI is required for the association of IQGAP1 with cdc42 or R-ras. Accordingly, FliI WT and FliI KND cells were plated on collagen for 60 or 240 min. Immunoblots prepared from IQGAP1 immunoprecipitates showed associations of IQGAP1 with cdc42 at 60 min and with R-ras at 240 min in FliI WT cells. These associations were 3- to 5-fold lower in FliI KND cells, suggesting that FliI enables the association of IQGAP1 with cdc42 and with R-ras (Figure 6B).

We examined further the role of FliI in the formation of short and long cell extensions. For these experiments, cdc42 or R-ras immunoprecipitates were prepared from FliI WT or FliI KND cells that had been plated for 60 min (cdc42) or 240 min (R-ras) on collagen or had been maintained in suspension without attachment to the collagen matrix. IQGAP1 associated with cdc42 in FliI WT cells, but this association was >6-fold weaker in FliI KND cells, suspended cells, or in immunoprecipitates prepared with a control antibody ($p < 0.01$; Figure 6C). Similarly, R-ras immunoprecipitates prepared from lysates collected at 240 min after plating showed an association between R-ras and IQGAP1 in FliI WT cells, but not in FliI KND cells or cells maintained in suspension (Figure 6D).

Arising from the apparently central role of FliI in enabling the function of cdc42 in the formation of cell extensions, we examined the formation of short and long cell extensions in FliI WT and FliI KND cells. Confocal images showed reduced numbers of small and long cell extensions in FliI KND cells compared with FliI WT cells (Supplemental Figure S2A). These results were similar to the data obtained with IQGAP1+/+ and IQGAP1–/– cells (Figure 4A). We next examined the role of cdc42 in the formation of short extensions in FliI cells. In FliI WT or KND cells transfected with HA-cdc42 DN or control vector, there was enhanced development of short cell extensions at 20–60 min, which in cells transfected with control vector, gradually decreased at 240 min ($p < 0.01$) and 360 min ($p < 0.01$). Cells that were transfected with HA-cdc42-DN consistently exhibited reduced numbers of short extensions throughout the sampling period (Supplemental Figure S2B). In control cells there was a gradual, time-dependent increase of the number of long cell extensions, whereas cell extension development was markedly reduced in HA-cdc42-DN cells. Cells that were transfected with HA-R-ras-DN or the control vector exhibited similar numbers of short cell extensions over 20–360 min (Supplemental Figure S2C), suggesting that R-ras is not involved in the formation of short extensions. In contrast, the number of long cell extensions progressively increased over time in control cells compared with cells transfected with HA-R-ras-DN that showed limited formation of long extensions ($p < 0.01$; Supplemental Figure S2C). These data indicate that in FliI cells, the collective activities of cdc42 and R-ras are required for the development of short cell extensions which then develop into long cell extensions.

Requirement of IQGAP1 for FliI interactions with cdc42 and R-ras

We determined whether IQGAP1 is required for FliI interactions with cdc42 or R-ras. IQGAP1+/+ and IQGAP–/– cells were plated on collagen and lysed. The lysates were immunoprecipitated with a FliI antibody and the immunoprecipitates were immunoblotted for cdc42 or R-ras. In the absence of IQGAP1 expression, there was > 5-fold reduced association of FliI with cdc42 or R-ras at 60 min or 240 min after plating ($p > 0.01$; Figure 7A).

Since we had observed that the LRR of FliI (but not the GLDs) of FLiI interacts with IQGAP1 (Figure 2), we examined whether the LRR of FliI is also necessary for interactions with cdc42 and R-ras. IQGAP1+/+ or IQGAP1–/– cells were transfected with HA-FLiI LRR or HA-empty vector and the transfected cells were then plated on collagen. Lysates were collected at 60 and 240 min after plating and immunoprecipitated with HA antibody. In these experiments, IQGAP1+/+ cells transfected with HA-FliI-LRR showed associations of the FliI-LRR with cdc42 and R-ras, whereas HA-FliI-LRR-transfected IQGAP–/– cells showed fourfold lower associations ($p < 0.01$; Figure 7B).

Collagen remodeling

When plated on collagen, fibroblasts form extensions that tunnel through collagen pores (Martins and Kolega, 2006) and by application of tractional forces, compact and align the collagen fibrils that surround the cell. For quantification of this process, 5 h after plating of cells, collagen matrices were imaged by reflectance confocal microscopy. Collagen compaction in ROI around cell extensions and cell-induced collagen fiber alignment was measured as described (Mohammadi *et al.,* 2014). FliI KND cells showed 1.5-fold ($p < 0.01$) lower compaction of collagen fibrils (measured in the ROI around cells) and 1.5-fold ($p < 0.01$) reduction of collagen fibril alignment compared with WT cells (Figure 8A). Similarly, IQGAP null cells show 1.2-fold ($p < 0.01$) and 1.5-fold ($p < 0.01$) reduction in collagen compaction and collagen alignment (Figure 8B).

In a rescue experiment in which IQGAP1–/– cells were transfected with GFP-IQGAP1, there was a 1.1-fold increase ($p < 0.01$) in collagen compaction and a 1.5-fold ($p < 0.01$) increase in collagen alignment in those IQGAP1–/– cells that were transfected with GFP-IQGAP1 (Figure 8C). For assessing the impact of cdc42 and R-ras on collagen remodeling we transfected IQGAP1+/+ cells transfected with GFP-cdc42 DN or GFP-R-ras DN. When these cells were plated on fibrillar collagen, there was a 1.6-fold ($p < 0.01$) and 1.5-fold ($p < 0.01$) reduction in collagen compaction and collagen alignment in those cells transfected with the DN GFP-cdc42 or the DN GFP-R-ras (Figure 8D).

DISCUSSION

The molecules that regulate the formation of the cell extensions required for the remodeling of collagen are not defined. FliI, by virtue of its multidomain structure (Liu and Yin, 1998), performs two quite separate functions (Arora *et al.,* 2018). The GLDs are involved in actin cytoskeletal rearrangements while the LRR region may regulate signal transduction through its association with R-ras. Here we show that FliI also acts as an adaptor protein to bind IQGAP1 and co-ordinates with cdc42 and R-ras (Figure 9) to control cell extension formation from nascent cell extensions. In fibroblasts, these cell extensions enlarge over time and are involved in binding and remodeling collagen by application of tractional forces.

IQGAP1 and cell extensions

We found that in fibroblasts, IQGAP1 associates with FliI and colocalizes at cell adhesion sites to regulate the development of

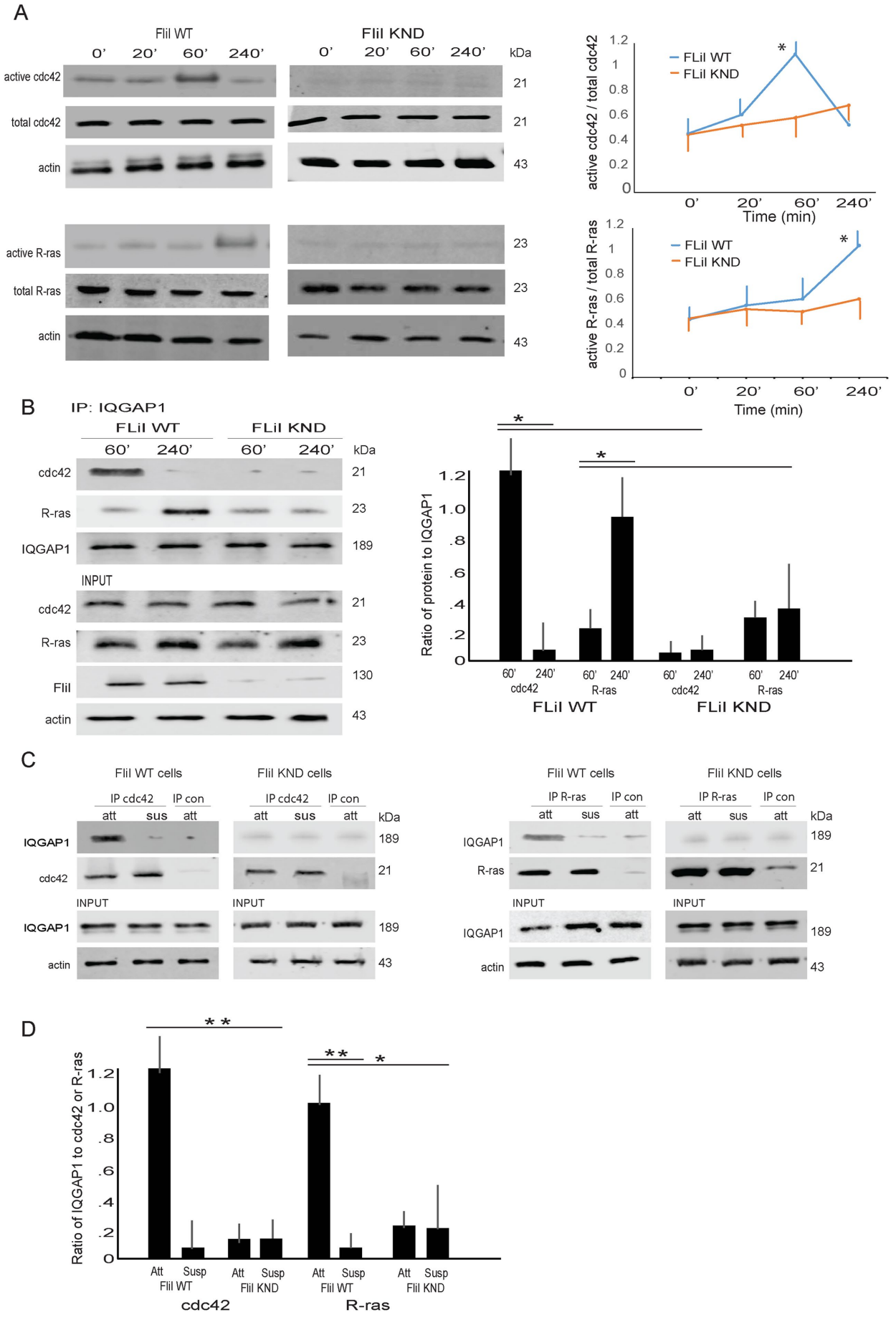
A
Flil WT
Flil KND
0'
20'
60'
240'
kDa
active cdc42
total cdc42
actin
21
21
43
active R-ras
total R-ras
actin
23
23
43
active cdc42 / total cdc42
FLil WT
FLil KND
Time (min)
active R-ras / total R-ras
FLil WT
FLil KND
Time (min)
B
IP: IQGAP1
FLil WT
FLil KND
cdc42
R-ras
IQGAP1
INPUT
cdc42
R-ras
Flil
actin
21
23
189
21
23
130
43
Ratio of protein to IQGAP1
cdc42
R-ras
cdc42
R-ras
FLil WT
FLil KND
C
Flil WT cells
Flil KND cells
IP cdc42
IP con
att
sus
att
IQGAP1
cdc42
INPUT
IQGAP1
actin
kDa
189
21
189
43
Flil WT cells
Flil KND cells
IP R-ras
IP con
IQGAP1
R-ras
INPUT
IQGAP1
actin
189
21
189
43
D
Ratio of IQGAP1 to cdc42 or R-ras
Att
Susp
Flil WT
Flil KND
cdc42
R-ras

actin-rich cell extensions. IQGAP1 contains several protein-interacting domains and acts as a scaffolding protein, which enables binding to a diverse array of signaling and structural molecules to integrate cytoskeletal and adhesion mechanisms with signaling networks (Briggs and Sacks, 2003; Mateer *et al.,* 2003). IQGAP1 modulates cross-talk between diverse pathways that mediate signaling by Rho family GTPases and calmodulin (Li and Sacks, 2003). Similar to previous reports, we found that in cells spreading on collagen, IQGAP1 associates with and activates cdc42 to induce filopodia formation (Swart-Mataraza *et al.,* 2002). Further, the GRD of IQGAP1 (Mataraza *et al.,* 2003) is required for these activities. In this context, IQGAP1, through its actin filament-binding site, regulates filopodia formation in spreading cells by modulating the organization and assembly of actin filaments (Fukata *et al.,* 1997). In addition, we found that IQGAP1 expression is required for the association of the LRR domain of FliI with cdc42 and R-ras. Evidently, IQGAP1 and FliI, which both play important adaptor functions in cells, also require each other and their mutual binding to ensure appropriate spatio-temporal control of actin assembly and, as a result, the formation of cell extensions.

It is thought that cdc42 regulates the formation of thin, fragile, and long cell extensions (20–30 μm) (Kornberg and Roy, 2014). These particular extensions, which resemble cytonemes and are involved in developmental processes, are sensitive to chemical and physical stress, are devoid of actin bundles, assist spreading cells in adhesion, and are involved in long-distance intercellular signaling (Koizumi *et al.,* 2012; Yamashita *et al.,* 2018). In contrast to the features of these cytoneme-like structures, we found actin-rich, physically robust extensions 4–20 μm in length that develop in spreading fibroblasts and contribute to collagen remodeling. We used Myo-10 as a tip marker (Berg *et al.,* 2000; Berg and Cheney, 2002) to facilitate the measurement of the lengths of these cell extensions. Notably, molecular motors such as myosin-X maintain the stability of filopodia, help to transport proteins long distance, and probe the pericellular microenvironment (Jacquemet *et al.,* 2015). The morphology and function of these extensions are consistent with earlier in vivo data from rodent models (Melcher and Chan, 1981; Everts *et al.,* 1996), which show the importance of long cell extensions in collagen remodeling. Until the conduct of the current experiments, the signaling molecules that regulate the formation of these cell extensions have not been well defined.

We found that IQGAP1 interacts with R-ras to promote the formation of long extensions, which arise by maturation from shorter extensions, a process that is regulated by an association between IQGAP1 and cdc42. This previously unrecognized association involving IQGAP1 and R-ras (Morgan *et al.,* 2019) in fibroblasts suggests that IQGAP1 provides a scaffolding function needed for activation of R-ras (but not K-Ras, H-Ras, or N-Ras), which in turn is required for the formation of long cell extensions. Notably, when R-ras is recruited to the leading edge of migrating cells, it regulates cell adhesion to collagen by modulating β1 integrin affinity and avidity (Keely *et al.,* 1999; Wozniak *et al.,* 2005; Conklin *et al.,* 2010). While IQGAP1 is clearly essential for cell extension formation, FliI evidently provides critical adaptor functions that link IQGAP1, R-ras, and cdc42 in space and time.

Requirement for FliI

We examined the role of FliI in enabling IQGAP1 interactions with cdc42 and R-ras using fibroblasts from mice with stable KND of FliI. These cells showed equivalent expression levels of IQGAP1, cdc42, and R-ras. FliI colocalized with IQGAP1 in immunostaining and bound in co-immunoprecipitation studies; pull-down experiments showed specific associations between IQGAP1 and the FliI-LRR but not the FliI-GLD domain. These findings are consistent with the multifunctional nature of FliI (Liu and Yin, 1998; Arora *et al.,* 2018), a member of the gelsolin family of proteins. Whereas the actin capping activity of FliI regulates actin remodeling through its GLD, its LRR region acts as an adaptor to integrate the functions of proteins involved in signaling. Notably, the LRR of FliI exhibits an amino acid sequence that is similar to the amino acid sequences of LRR domains in other proteins that are involved in functions that regulate cell adhesion and Ras signaling (Campbell *et al.,* 1993). Thus, while FliI is a very low abundance actin-binding protein, knockout of FliI in mice is embryonic lethal (Campbell *et al.,* 2002). Accordingly, adaptor functions played by FliI in cell signaling may be relatively more important than its GLDs in the context of mammalian connective tissue development and remodeling.

We found that in FliI WT cells plated on collagen, there was increased cdc42 and R-ras activity at 60 and 240 min, which was contemporaneous with maximum growth of short and long cell extensions, respectively. A consistent finding in our experiments was the FliI-dependent association between IQGAP1 and cdc42, a process

FIGURE 6: Involvement of FliI and IQGAP1 in mediating association with cdc42 and R-ras. (A) FliI WT and KND cells were plated on collagen from 0 to 240 min. Top panels, active and total cdc42. Bottom panels, active and total R-ras. Densitometric analysis of active and total cdc42 and R-ras were expressed as ratios. Time course data are shown in the line plot (right panels). Data are mean ± SD of four independent samples. Activation of cdc42 and R-ras was different between FliI WT and Fli KND cells at 60 min (for cdc42) and 360 min (for R-ras; $*p < 0.01$ by ANOVA). (B) Effect of FliI expression on association of IQGAP1 with cdc42 or R-ras. FliI WT and FliI KND cells were plated on collagen for 60 or 240 min. Lysates were immunoprecipitated with IQGAP1 antibody. IQGAP1 immunoprecipitates were immunoblotted for cdc42 or R-ras and analyzed by densitometry. Data in histograms in right panels are ratios of blot densities of cdc42 to IQGAP1 or of R-ras to IQGAP1. Data are mean ± SD of four independent samples. Differences in ratios of cdc42 and R-ras to IQGAP1 were analyzed by ANOVA. Differences between cdc42 or R-ras groups are shown by horizontal lines above histogram bars ($*p < 0.01$). (C) Effect of cell attachment to collagen and FliI expression on association of IQGAP1 with cdc42 and R-ras. Left panels: FliI WT or FliI KND cells were plated on collagen for 60 min or maintained in suspension to prevent matrix interactions. Lysates were immunoprecipitated with cdc42 antibody or a control antibody (nebulin). The immunoprecipitates were immunoblotted for IQGAP1. Right panels: FliI WT or FliI KND cells were plated on collagen for 240 min or maintained in suspension to prevent matrix interactions. Lysates were immunoprecipitated with R-ras antibody or a control antibody (nebulin). The immunoprecipitates were immunoblotted for IQGAP1. (D) Data in histogram are ratios of blot densities of IQGAP1 either to cdc42 or to R-ras for FliI WT or FliI KND cells. Data are mean ± SD of four independent samples for each experimental condition. Differences in ratios were analyzed by ANOVA. Differences within cdc42 or R-ras groups are shown by horizontal lines above histogram bars ($**p < 0.01$; $*p < 0.05$).

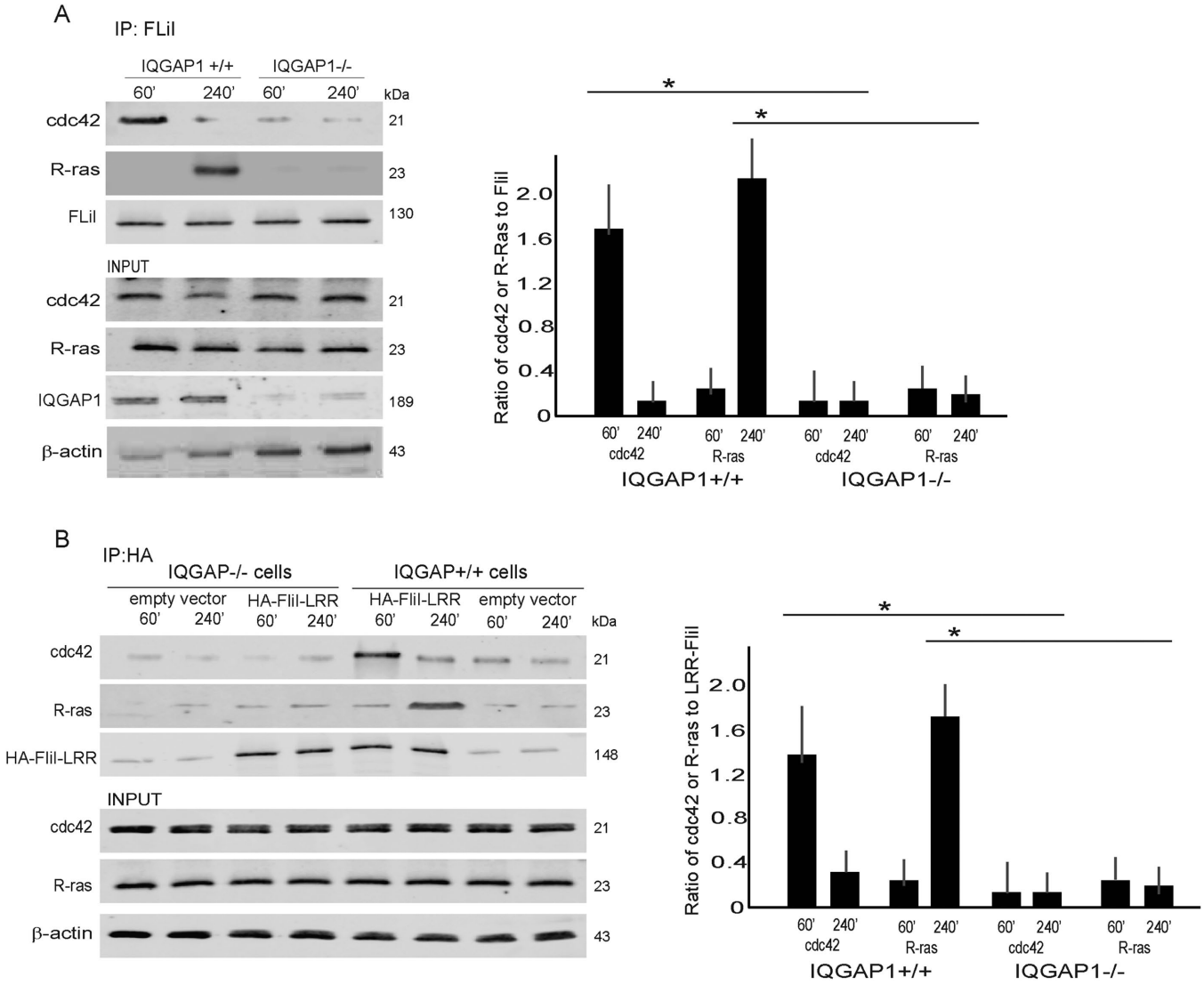

FIGURE 7: Involvement of IQGAP1 in association of Flil-LRR with cdcC2 or R-ras. (A) IQGAP1+/+ and IQGAP1–/– cells were plated on collagen. Cell lysates were collected at 60 or 240 min and immunoprecipitated with Flil antibody. Panels on left show immunoblots of cell lysates and of Flil-immunoprecipitated proteins. The blot densities from the immunoprecipitations were measured and expressed as ratios of cdc42 to Flil or of R-ras to Flil. The ratios for the IQGAP1+/+ and IQGAP1–/– cells are shown in the histogram on the right. Data are mean ± SD of four independent samples for each experimental condition. Differences in ratios were analyzed by ANOVA. Differences within cdc42 or R-ras groups are shown by horizontal lines above histogram bars (*$p < 0.01$). (B) IQGAP1+/+ and IQGAP1–/– cells were transfected with HA-Flil LRR or HA empty vector. Cells were plated on collagen for 60 or 240 min. Lysates collected from transfected cells were immunoprecipitated with HA antibody. Immunoblots of total cell lysates and of immunoprecipitates are shown in left panels. The blot densities from the immunoprecipitations were measured and expressed as ratios of cdc42 to Flil or of R-ras to Flil-LRR. The ratios for the IQGAP1+/+ and IQGAP1–/– cells are shown in the histogram on the right. Data are mean ± SD of four independent samples for each experimental condition. Differences in ratios were analyzed by ANOVA. Differences within cdc42 or R-ras groups and between IQGAP1+/+ cells and IQGAP1–/– cells are shown by horizontal lines above histogram bars (*$p < 0.01$).

that requires integrin engagement with collagen. Evidently, in addition to providing temporo-spatial control of the associations of IQGAP1, R-Ras, and cdc42, Flil also links these proteins spatially to nascent cell adhesions, which thereby focuses their actin-regulating activities at sites of developing cell extensions. Indeed, the formation of these extensions was greatly attenuated in Flil KND cells. Thus, Flil acts as an integrin-dependent adaptor that promotes the functional associations of IQGAP1 with cdc42 and R-ras. Therefore Flil, like other actin capping proteins that are involved in controlling the stochastic dynamics of actin-rich cell extensions and which are used by cells to probe their microenvironment (Zhuravlev and Papoian, 2009), also plays fundamental roles in linking cell adhesion, cell extension formation, and collagen remodeling into an integrated series of processes (Kopecki *et al.*, 2007; Mohammad *et al.*, 2012).

We conclude that in addition to its role as an actin capping and severing protein, Flil acts as an adaptor protein to bind IQGAP and co-ordinate with cdc42 and R-ras to control cell extension formation from nascent, short extensions. These longer cell extensions play an important role in binding to and remodeling fibrillar ECM proteins like collagen.

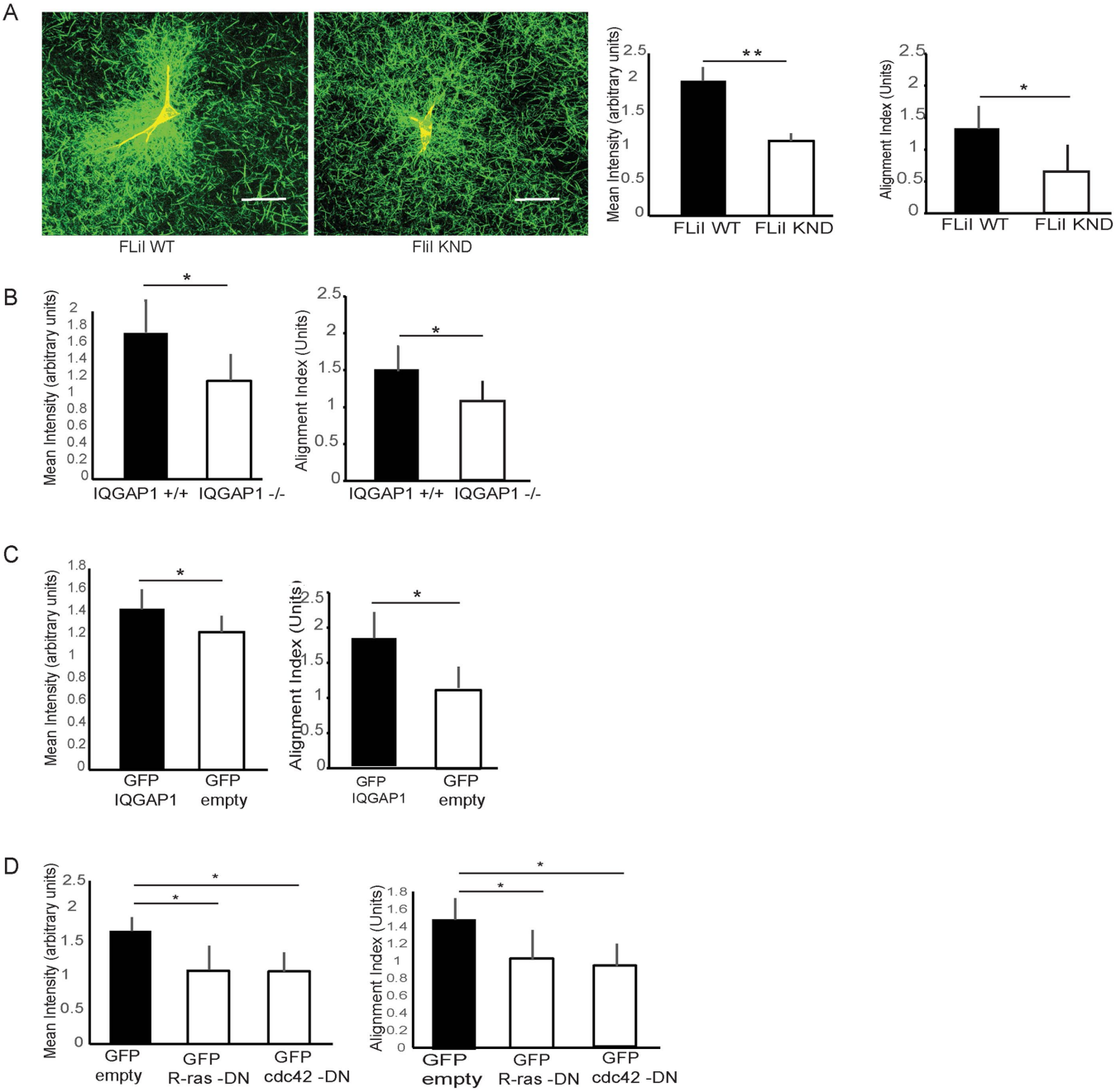

FIGURE 8: (A) Summed projection of optical sections (nominal 2 μm in thickness) obtained by confocal imaging show collagen remodeling by tractional forces from Flil WT and Flil KND cells plated on fibrillar type I collagen for 5 h. Scale bar, 40 μm. Histograms to the right of images show mean collagen fluorescence intensity in the ROI (2 μm × 2 μm sampling grid) measured around cell peripheries from reflectance confocal images (mean intensity; left histogram) and the collagen alignment index was measured along cell extensions (right histogram). All data are mean ± SD of intensities of collagen fluorescence or of collagen alignment indices, as described in *Materials and Methods*. Data comparisons between two groups were analyzed by Student's *t* test. For comparisons between three groups (D, below), ANOVA was used. Differences between groups are shown by $*p < 0.05$ or $**p < 0.01$. (B) IQGAP1+/+ and IQGAP1–/– cells were plated for 5 h on collagen and analyzed identically as described for A. (C) IQGAP1–/– cells were transfected with GFP-IQGAP1 or GFP empty vector and analyzed as described above. (D) IQGAP1+/+ cells were transfected with GFP empty vector or GFP-cdc42 DN or GFP-R-ras DN and plated on fibrillar collagen for 5 h and analyzed as described above.

MATERIALS AND METHODS

Reagents

Rabbit monoclonal antibody to Flil was from Epitomics (Burlington, CA). The protease inhibitor cocktail, nebulin antibody, RIPA buffer, β-actin antibody (clone AC-15), myosin10 antibody, and fluorescein isothiocyanate–conjugated goat anti-mouse antibody and tetramethyl rhodamine isothiocyanate-phalloidin were obtained from Sigma-Aldrich (Oakville, ON, Canada). Monoclonal antibodies to Flil and IQGAP1 were purchased from Santa Cruz. As additional monoclonal antibody to IQGAP1 and polyclonal antibodies to

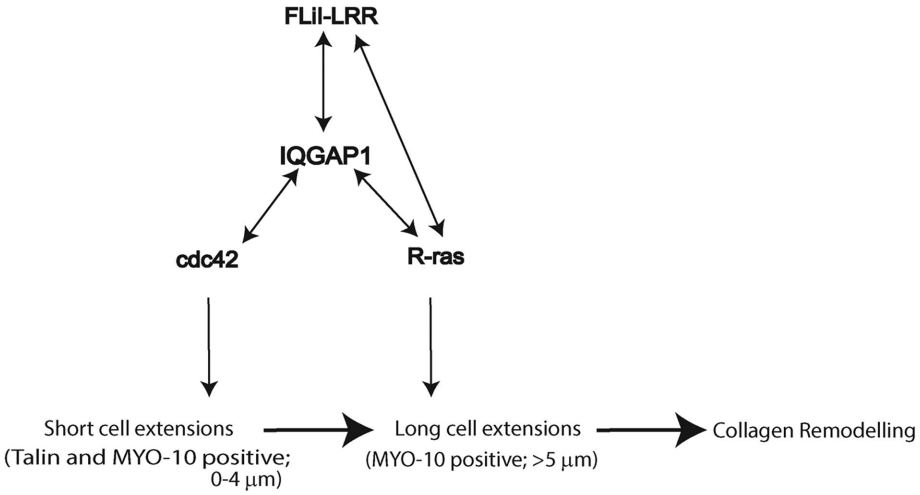

FIGURE 9: Diagram showing the proposed interaction between FliI and IQGAP1 and FliI and R-Ras that co-ordinates cdc42 and R-ras in controlling the formation of cell extensions from nascent adhesions. 1) IQGAP1 regulates cdc42 to mediate cdc42-induced formation of short cell extensions, which later develop into long cell extensions. 2) IQGAP1 co-ordinates with R-ras to enable the growth of short extensions into longer cell extensions, which is dependent on the LRR of FliI.

IQGAP2 and IQGAP3 were obtained from Abcam. Protein G beads and protein Sepharose glutathione beads were purchased from Dynamed. Glutathione Sepharose beads were from Sigma, Aldrich (Oakville, ON, Canada). On-Target siRNA to IQGAP1 was purchased from GE Dharmacon (Mississauga, ON, Canada). Type 1 bovine collagen was purchased from Advanced BioMatrix (Carlsbad, CA).

Cell culture

WT and knock-down (KND) FliI mouse fibroblasts were obtained from 3T3 fibroblasts as we described (Mohammad *et al.*, 2012). Briefly, for preparation of FliI stable cell lines, the following oligonucleotides were synthesized: top strand-5′-gatccGAAGATA CACACTATGTTATTCAAGAGATAACATAGTGTGTA-TCTTCTTTTTTA CGCGTg-3′ and bottom strand-5′aattcACGCGTA AAAAAGAAGATACACACTATGTTATCTCTTGAATAACATAGTGT-GTA TCTTCg-3′

These sequences correspond to the sense 5′-GAAGATACACAC-TATGTTA-3′ and antisense 5′-TAACATAGTGTGTATCTTC-3′ for mouse FliI; they were annealed and inserted into an RNAi-Ready pSIREN-RetroQ-DsRed-Express vector (Clontech) at BamHI/EcoRI sites. Insert sequences were confirmed by sequencing. The plasmid was cotransfected with pVSV-G into GP-293 cells for retrovirus production. NIH-3T3 cells were infected with the virus; 2 wk later, the transfected cells were sorted in phosphate-buffered saline (PBS)/0.5% fetal bovine serum (FBS) (Beckman-Coulter Altra flow cytometer/sorter). Cells with strong red fluorescence were cloned by limiting dilution. Oligonucleotides (top strand 5′-gatccgtgcgttgc-tagtaccaacttcaagagatttttttacgcgtg-3 and bottom strand 5′-aattcac-gcgtaaaaaatctcttgaagttggtactagcaacgcacg-3′ containing only the sense strand of WT FliI 5′-GTGCGTTGCTAGTACCAA-3′) were annealed and inserted into the same vector to establish control cell lines. FliI KND and control cell lines were subsequently established. FliI KND cell lines were confirmed by immunoblotting for FliI.

IQGAP+/+ (WT) and IQGAP1–/– (null) MEFs cells were provided by one of us (D.B.S.) (Li *et al.*, 2000; Ren *et al.*, 2007). Briefly, MEFs were isolated from 14-day embryos of IQGAP–/– mice (Li *et al.*, 2000) and normal littermate controls. For immortalization, primary cultures of MEFs were transfected with simian virus 40 large T antigen, and cultured to grow single colonies. Cells were cultured at 37°C in complete DMEM containing 10% FBS and 10% antibiotics (124 U/ml penicillin G, 50 μg/ml gentamicin sulfate, and 0.25 μg/ml Fungizone). Cells were maintained in a humidified incubator containing 95% air and 5% CO_2 and passaged with 0.01% trypsin (Life Technologies, Burlington, ON).

Colocalization of proteins

Fibroblasts were plated on Glass Bottom Microwell dishes (35 mm petri dishes, 14 mm microwell No. 1.5 cover-glass; MatTek Corp.) and incubated for 2.5 hrs at 37°C. Cells were fixed with 4% paraformaldehyde in PBS for 10 min, permeabilized with 0.3% Triton X-100 for 10 min, and blocked with CAS-Block (Life Technologies) for 20 min at room temperature. Cells were incubated with appropriate primary and fluorescent secondary antibodies diluted in 0.03% Triton X-100, both for 1 h at 37°C. Confocal microscopy (×40 oil-immersion lens; Leica TCS SP8, Heidelberg, Germany) was used to localize proteins of interest in specific regions within cells that are outlined for specific experiments. For quantification of the immunostained proteins, the Pearson coefficient of double-stained samples was computed using ImageJ to quantify the extent of colocalization (Bolte and Cordelieres, 2006).

PBD and RBD pull downs

In pull-down experiments for measuring active cdc42 and R-ras, we used GST-PBD and GST-RBD beads. Experiments were performed by lysing adherent or suspended fibroblasts in buffer (50 mM Tris, pH 7.6, 500 mM NaCl, 1% Triton X-100, 0.1% SDS, 0.5% deoxycholate, 10 mM $MgCl_2$, 200 mM orthovanadate, and protease inhibitors). In one of the experiments GFP-immunoprecipitates were eluted with elution buffer (50 mM Tris, pH 7.6, 1.5% Triton X-100, 10 mM $MgCl_2$, 0.5 mM deoxycholate, and 0.1% SDS with protease inhibitors). Lysates were clarified by centrifugation, equalized for total volume and protein concentration, and rotated for 30 min with 30 μg of purified GST-PBD or RBD bound to glutathione Sepharose beads. The bead pellets were washed in a buffer solution (50 mM Tris, pH 7.6, 150 mM NaCl, 1% Triton X-100, 10 mM $MgCl_2$, protease inhibitors) and the proteins were separated by SDS–PAGE.

Purification of FliI recombinant proteins

GST-tagged proteins expressed in bacterial expression systems were isolated and purified by adapting earlier methods (Frangioni and Neel, 1993). Briefly, BL21 (DE3) cells were transformed with FliI-LRR and FliI GLD constructs. Luria broth (250 ml) containing ampicillin (100 μg/ml) was inoculated at 1:50 ratio from overnight bacterial culture containing the FliI construct. The culture was grown at 37°C followed by induction with IPTG (1 mM) for 3.5 h. Proteins isolated from inclusion bodies in STE buffer (10 mM Tris, pH 8.0; 150 mM NaCl, 1 mM EDTA, 1.5% Sarkosyl, and 5 mM dithiotheitol) were dialyzed overnight and incubated with glutathione Sepharose beads (Pharmacia) followed by washing 3× with STE buffer without Sarkosyl.

Immunoblotting and immunoprecipitation

Cell extracts were prepared by scraping cells into lysis buffer (50 mM Tris, pH 7.5; 150 m1M NaCl; 1% Triton X-100; 0.1% SDS; 1% sodium deoxycholate, and a 1:50 dilution of protease inhibitor cocktail; Sigma). The homogenate was centrifuged at 10,000 rpm for 4 min and the supernatant was separated for analysis. BCA analysis was conducted to ensure equal amounts of protein, which was separated on SDS–PAGE gels and transferred to nitrocellulose membranes. Membranes were blocked with 1% bovine serum albumin in TBS overnight and incubated with appropriate primary and secondary antibodies diluted in Tris-buffered saline (TBS) with 0.01% Tween-20 for 1 h at room temperature. For immunoprecipitation, FliI WT and KND were plated on collagen for an hour. Washed samples were scraped into RIPA buffer (Sigma). The supernatants of centrifuged samples were incubated with FliI antibody (Epitomics) or IQGAP antibody followed by the addition of equivalent amounts of protein A Sepharose beads (Pierce, Thermo Scientific). Immunoblotted samples were probed with appropriate antibodies and secondary antibodies and blots were imaged with a Li-Cor imaging system (Mandel, Toronto, ON, Canada).

Collagen remodeling and quantification

For analysis of collagen remodeling by tractional forces, we used coverslips (25 mm, VWR) that were sterilized with UV light (10 min), submerged in 2% 3-aminopropyltrimethoxysilane (Sigma-Aldrich) for 15 min, washed three times with distilled water, immersed in 0.1% glutaraldehyde (Caledon Laboratories, ON, Canada) for 15 min, washed three times with distilled water, air-dried for 10 min, and coated with collagen, which polymerized for an hour at 37°C. Cells were plated on these collagen-coated substrates for 5 h before fixation with 4% paraformaldehyde for 10 min and permeabilized with 0.3% Triton X-100 for 10 min. Coverslips were inverted on to glass bottom dishes with mounting medium. Confocal reflectance microscopy was used to visualize and subsequently quantify collagen fiber orientation as described (Mohammadi *et al.*, 2015). Images of fibrillar collagen were quantified to provide estimates of the remodeling activity using reorganization (alignment index) of collagen fibers around cell extensions.

The abundance of collagen fibrils immediately surrounding cell extensions (i.e., a measure of collagen compaction) was determined by creating 2 µm × 2 µm square sampling grids in the ROI and the fluorescence intensity attributable to the reflected collagen fibrils was analyzed using ImageJ. Altogether, 20 cells were measured for each experimental condition. Collagen fiber alignment with respect to cell extensions was quantified in ROI in fixed areas around cell extensions (in vitro) using Fast Fourier Transform and Oval Profile (ImageJ plug-in) as described earlier (Mohammadi *et al.*, 2014). The alignment index was defined based on higher pixel intensities in a specific angle, which were related to the orientation of collagen fibers in the corresponding direction. These signals were quantified by calculation of area under the intensity curve within ±10 degrees of the peak using an in-house written C++ code.

Mass spectrometry

For mass spectrometry analysis of FliI immunoprecipitates, cells were lysed on ice and supernatants from centrifuged samples were incubated with FliI antibody for 1 h followed by the addition of protein A Sepharose beads (Pierce, Thermo Scientific). Proteins associated with beads were eluted with 50 mM glycine buffer (pH 2.3–2.5). The pH of the eluted proteins was increased to near physiological pH by dialysis for 36 h in carbonate buffer (25 mM NH_4HCO_3; pH = 7.5). The dialyzed samples were treated with trypsin (0.1 µg/µl, Roche, Indianapolis, IN) and rotated overnight at 37°C overnight. Subsequently, 0.1% acetic acid was added to the sample followed by air-drying with an evaporator. Lyophilized samples were analyzed by LC-MS/MS (SPARC Mass Spectrometry Facility, Hospital for Sick Children, Toronto, ON, Canada).

Statistical analysis

For all continuous variable data, means, standard deviations, and in some instances, standard errors of the means, were computed. When appropriate, comparisons between two samples were made by Student's *t* test with statistical significance set at $p < 0.05$. For multiple comparisons, ANOVA was used followed by Tukey's test for assessment of individual differences. All experiments were performed at least three times on different days and each experiment was conducted in triplicate.

ACKNOWLEDGMENTS

This work was supported by Canadian Institute of Health Research operating grant to C.A.M. (MOP-36332). C.A.M. is supported by Canada Research Chair (Tier 1). The funders had no role in the study design, data collection and analysis, decision to publish, or preparation of the manuscript. D. Sacks is supported by the Intramural Research Program of the National Institutes of Health.

REFERENCES

Arora PD, He T, Ng K, McCulloch CA (2018). The leucine-rich region of Flightless I interacts with R-ras to regulate cell extension formation. Mol Biol Cell 29, 2481–2493.

Arora PD, Wang Y, Bresnick A, Janmey PA, McCulloch CA (2015). Flightless I interacts with NMMIIA to promote cell extension formation, which enables collagen remodeling. Mol Biol Cell 26, 2279–2297.

Berg JS, Cheney RE (2002). Myosin-X is an unconventional myosin that undergoes intrafilopodial motility. Nat Cell Biol 4, 246–250.

Berg JS, Derfler BH, Pennisi CM, Corey DP, Cheney RE (2000). Myosin-X, a novel myosin with pleckstrin homology domains, associates with regions of dynamic actin. J Cell Sci 113 (Pt 19), 3439–3451.

Bolte S, Cordelieres FP (2006). A guided tour into subcellular colocalization analysis in light microscopy. J Microsc 224, 213–232.

Bonnans C, Chou J, Werb Z (2014). Remodelling the extracellular matrix in development and disease. Nat Rev Mol Cell Biol 15, 786–801.

Bourguignon LY, Gilad E, Rothman K, Peyrollier K (2005). Hyaluronan-CD44 interaction with IQGAP1 promotes Cdc42 and ERK signaling, leading to actin binding, Elk-1/estrogen receptor transcriptional activation, and ovarian cancer progression. J Biol Chem 280, 11961–11972.

Briggs MW, Sacks DB (2003). IQGAP proteins are integral components of cytoskeletal regulation. EMBO Rep 4, 571–574.

Brown MD, Sacks DB (2006). IQGAP1 in cellular signaling: bridging the GAP. Trends Cell Biol 16, 242–249.

Campbell HD, Fountain S, McLennan IS, Berven LA, Crouch MF, Davy DA, Hooper JA, Waterford K, Chen KS, Lupski JR, *et al.* (2002). Fliih, a gelsolin-related cytoskeletal regulator essential for early mammalian embryonic development. Mol Cell Biol 22, 3518–3526.

Campbell HD, Fountain S, Young IG, Claudianos C, Hoheisel JD, Chen KS, Lupski JR (1997). Genomic structure, evolution, and expression of human FLII, a gelsolin and leucine-rich-repeat family member: overlap with LLGL. Genomics 42, 46–54.

Campbell HD, Schimansky T, Claudianos C, Ozsarac N, Kasprzak AB, Cotsell JN, Young IG, de Couet HG, Miklos GL (1993). The Drosophila melanogaster flightless-I gene involved in gastrulation and muscle degeneration encodes gelsolin-like and leucine-rich repeat domains and is conserved in Caenorhabditis elegans and humans. Proc Natl Acad Sci USA 90, 11386–11390.

Conklin MW, Ada-Nguema A, Parsons M, Riching KM, Keely PJ (2010). R-Ras regulates beta1-integrin trafficking via effects on membrane ruffling and endocytosis. BMC Cell Biol 11, 14.

Davy DA, Campbell HD, Fountain S, de Jong D, Crouch MF (2001). The flightless I protein colocalizes with actin- and microtubule-based structures in motile Swiss 3T3 fibroblasts: evidence for the involvement of PI 3-kinase and Ras-related small GTPases. J Cell Sci 114, 549–562.

Dimchev G, Steffen A, Kage F, Dimchev V, Pernier J, Carlier MF, Rottner K (2017). Efficiency of lamellipodia protrusion is determined by the extent of cytosolic actin assembly. Mol Biol Cell 28, 1311–1325.
Everts V, van der Zee E, Creemers L, Beertsen W (1996). Phagocytosis and intracellular digestion of collagen, its role in turnover and remodelling. Histochem J 28, 229–245.
Frangioni JV, Neel BG (1993). Solubilization and purification of enzymatically active glutathione S-transferase (pGEX) fusion proteins. Anal Biochem 210, 179–187.
Fukata M, Kuroda S, Fujii K, Nakamura T, Shoji I, Matsuura Y, Okawa K, Iwamatsu A, Kikuchi A, Kaibuchi K (1997). Regulation of cross-linking of actin filament by IQGAP1, a target for Cdc42. J Biol Chem 272, 29579–29583.
Geiger B, Spatz JP, Bershadsky AD (2009). Environmental sensing through focal adhesions. Nat Rev Mol Cell Biol 10, 21–33.
Hall A (1998). Rho GTPases and the actin cytoskeleton. Science 279, 509–514.
Hall A (2005). Rho GTPases and the control of cell behaviour. Biochem Soc Trans 33, 891–895.
Hayashi H, Nabeshima K, Aoki M, Hamasaki M, Enatsu S, Yamauchi Y, Yamashita Y, Iwasaki H (2010). Overexpression of IQGAP1 in advanced colorectal cancer correlates with poor prognosis-critical role in tumor invasion. Int J Cancer 126, 2563–2574.
Jacquemet G, Hamidi H, Ivaska J (2015). Filopodia in cell adhesion, 3D migration and cancer cell invasion. Curr Opin Cell Biol 36, 23–31.
Jacquemet G, Humphries MJ (2013). IQGAP1 is a key node within the small GTPase network. Small GTPases 4, 199–207.
Kaibuchi K, Kuroda S, Amano M (1999). Regulation of the cytoskeleton and cell adhesion by the Rho family GTPases in mammalian cells. Annu Rev Biochem 68, 459–486.
Keely PJ, Rusyn EV, Cox AD, Parise LV (1999). R-Ras signals through specific integrin alpha cytoplasmic domains to promote migration and invasion of breast epithelial cells. J Cell Biol 145, 1077–1088.
Kobe B, Kajava AV (2001). The leucine-rich repeat as a protein recognition motif. Curr Opin Struct Biol 11, 725–732.
Koizumi K, Takano K, Kaneyasu A, Watanabe-Takano H, Tokuda E, Abe T, Watanabe N, Takenawa T, Endo T (2012). RhoD activated by fibroblast growth factor induces cytoneme-like cellular protrusions through mDia3C. Mol Biol Cell 23, 4647–4661.
Kopecki Z, Cowin AJ (2008). Flightless I: an actin-remodelling protein and an important negative regulator of wound repair. Int J Biochem Cell Biol 40, 1415–1419.
Kopecki Z, Luchetti MM, Adams DH, Strudwick X, Mantamadiotis T, Stoppacciaro A, Gabrielli A, Ramsay RG, Cowin AJ (2007). Collagen loss and impaired wound healing is associated with c-Myb deficiency. J Pathol 211, 351–361.
Kornberg TB, Roy S (2014). Cytonemes as specialized signaling filopodia. Development 141, 729–736.
Kwiatkowski DJ (1999). Functions of gelsolin: motility, signaling, apoptosis, cancer. Curr Opin Cell Biol 11, 103–108.
Kwong L, Wozniak MA, Collins AS, Wilson SD, Keely PJ (2003). R-Ras promotes focal adhesion formation through focal adhesion kinase and p130(Cas) by a novel mechanism that differs from integrins. Mol Cell Biol 23, 933–949.
Li Z, Sacks DB (2003). Elucidation of the interaction of calmodulin with the IQ motifs of IQGAP1. J Biol Chem 278, 4347–4352.
Li S, Wang Q, Chakladar A, Bronson RT, Bernards A (2000). Gastric hyperplasia in mice lacking the putative Cdc42 effector IQGAP1. Mol Biol Cell 20, 697–701.
Liu YT, Yin HL (1998). Identification of the binding partners for flightless I, A novel protein bridging the leucine-rich repeat and the gelsolin superfamilies. J Biol Chem 273, 7920–7927.
Martins GG, Kolega J (2006). Endothelial cell protrusion and migration in three-dimensional collagen matrices. Cell Motil Cytoskeleton 63, 101–115.
Mataraza JM, Briggs MW, Li Z, Entwistle A, Ridley AJ, Sacks DB (2003). IQGAP1 promotes cell motility and invasion. J Biol Chem 278, 41237–41245.
Mateer SC, Wang N, Bloom GS (2003). IQGAPs: integrators of the cytoskeleton, cell adhesion machinery, and signaling networks. Cell Motil Cytoskeleton 55, 147–155.
Melcher AH, Chan J (1981). Phagocytosis and digestion of collagen by gingival fibroblasts in vivo: a study of serial sections. J Ultrastruct Res 77, 1–36.
Mohammad I, Arora PD, Naghibzadeh Y, Wang Y, Li J, Mascarenhas W, Janmey PA, Dawson JF, McCulloch CA (2012). Flightless I is a focal adhesion-associated actin-capping protein that regulates cell migration. FASEB J 26, 3260–3272.
Mohammadi H, Arora PD, Simmons CA, Janmey PA, McCulloch CA (2015). Inelastic behaviour of collagen networks in cell-matrix interactions and mechanosensation. J R Soc Interface 12, 20141074.
Mohammadi H, Janmey PA, McCulloch CA (2014). Lateral boundary mechanosensing by adherent cells in a collagen gel system. Biomaterials 35, 1138–1149.
Morgan CJ, Hedman AC, Li Z, Sacks DB (2019). Endogenous IQGAP1 and IQGAP3 do not functionally interact with Ras. Sci Rep 9, 11057.
Nobes CD, Hall A (1995). Rho, rac, and cdc42 GTPases regulate the assembly of multimolecular focal complexes associated with actin stress fibers, lamellipodia, and filopodia. Cell 81, 53–62.
Noritake J, Watanabe T, Sato K, Wang S, Kaibuchi K (2005). IQGAP1: a key regulator of adhesion and migration. J Cell Sci 118, 2085–2092.
Ohta Y, Suzuki N, Nakamura S, Hartwig JH, Stossel TP (1999). The small GTPase RalA targets filamin to induce filopodia. Proc Natl Acad Sci USA 96, 2122–2128.
Rajalingam K, Schreck R, Rapp UR, Albert S (2007). Ras oncogenes and their downstream targets. Biochim Biophys Acta 1773, 1177–1195.
Ren JG, Li Z, Sacks DB (2007). IQGAP1 modulates activation of B-Raf. Proc Natl Acad Sci USA 104, 10465–10469.
Ridley AJ, Paterson HF, Johnston CL, Diekmann D, Hall A (1992). The small GTP-binding protein rac regulates growth factor-induced membrane ruffling. Cell 70, 401–410.
Self AJ, Caron E, Paterson HF, Hall A (2001). Analysis of R-Ras signalling pathways. J Cell Sci 114, 1357–1366.
Swart-Mataraza JM, Li Z, Sacks DB (2002). IQGAP1 is a component of Cdc42 signaling to the cytoskeleton. J Biol Chem 277, 24753–24763.
Wozniak MA, Kwong L, Chodniewicz D, Klemke RL, Keely PJ (2005). R-Ras controls membrane protrusion and cell migration through the spatial regulation of Rac and Rho. Mol Biol Cell 16, 84–96.
Yamashita YM, Inaba M, Buszczak M (2018). Specialized intercellular communications via cytonemes and nanotubes. Annu Rev Cell Dev Biol 34, 59–84.
Zhuravlev PI, Papoian GA (2009). Molecular noise of capping protein binding induces macroscopic instability in filopodial dynamics. Proc Natl Acad Sci USA 106, 11570–11575.